Monomer Substituent Effects in Catalytic Chain Transfer Polymerization: *tert*-Butyl Methacrylate and Dimethyl Itaconate

G. Evan Roberts, Thomas P. Davis,* and Johan P. A. Heuts*

Centre for Advanced Macromolecular Design, School of Chemical Engineering and Industrial Chemistry, The University of New South Wales, Sydney 2052, Australia

Graham E. Ball

NMR Facility and School of Chemical Sciences, The University of New South Wales, Sydney 2052, Australia

Received May 10, 2002; Revised Manuscript Received October 7, 2002

ABSTRACT: Kinetic and mechanistic studies have been performed on the cobaloxime-mediated catalytic chain transfer polymerization (CCTP) of *tert*-butyl methacrylate (*t*-BMA) and dimethyl itaconate (DMI) in order to further elucidate the role of monomer substituents in the hydrogen-abstraction reaction. The studies on *t*-BMA, which include a pulsed-laser polymerization study for the determination of the propagation rate coefficient, are inconclusive insofar that they cannot unambiguously distinguish between possible monomer viscosity effects and direct steric interactions between the substituents at the radical center and the cobalt catalyst in the hydrogen-abstraction reaction. Studies on the CCTP of DMI included ^{1}H, ^{13}C, COSY, NOESY, HMQC, and HMBC NMR studies of a mixture of DMI oligomers, which showed that the hydrogen abstraction occurs preferentially from the α substituent of the radical center rather than from the backbone yielding predominantly *E* isomers. The low chain transfer rate coefficient for DMI is conceivably caused by steric hindrances as a result of the large substituents.

Introduction

Over the past 2 decades, catalytic chain transfer (CCT) has been established as a convenient synthetic route to macromonomers.[1] Although many studies have been performed on the mechanism of CCT, certain aspects still remain open to conjecture. In a number of recent publications the possibility that the CCT reaction rate is diffusion-controlled has been discussed.[2−6] The experimental evidence to support a diffusion-controlled hypothesis in methacrylate polymerization comes from a number of sources. First, the CCT reaction in methacrylates is assumed to be a bimolecular radical−radical interaction leading to H-abstraction, with a measured rate coefficient of about 10^7 dm^3 mol^{-1} s^{-1}; similar radical−radical disproportionation reactions in free-radical polymerization, characterized by similar rate coefficients, are known to be diffusion-controlled.[7] Second, the experimental Arrhenius parameters for the chain transfer coefficients for methyl (MMA), ethyl (EMA), and butyl methacrylate (BMA) are consistent with diffusion control.[2] Third, variations in the measured chain transfer constants (C_S) for different cobaloximes have been tentatively explained by differences in the cross-sectional area of these square planar complexes, with larger cobaloximes displaying lower chain transfer constants.[8] Finally, there is a significant difference in C_S for a homologous series of *n*-alkyl methacrylates, with C_S decreasing in magnitude as the ester chain length increases.[2,3,6,9,10] It was found that all studied methacrylates in our group to date (with monomer viscosities ranging from 0.37 to 2.50 cP at 60 °C),[2,3,6] with the exception of 3-[tris(trimethylsilyloxy)-silyl]propyl methacrylate (where poor control of experimental conditions prohibited careful kinetic studies), display a roughly inverse relationship between the chain transfer rate coefficient (k_{tr}) and the monomer viscosity (eq 1)

$$k_{tr}\eta_{monomer} = C_S k_p \eta_{monomer} \approx \text{constant} \qquad (1)$$

where $\eta_{monomer}$ is the bulk monomer viscosity and k_p is the propagation rate coefficient. Subsequent studies in which bulk viscosity was changed by addition of high molecular polymer (i.e., causing a viscosity increase) and by addition of a low viscosity solvent (i.e., causing a viscosity decrease) showed that changes in bulk medium viscosity do not change the chain-transfer rate.[6,10] This in turn has led to the conclusion that microscopic effects on the molecular scale are responsible for the observed changes in chain transfer rate coefficient with changing substituents in the methacrylate. The available experimental data to date do not allow for a discrimination between the two possibilities that these changes are caused by changes in microscopic viscosity (i.e., changes in monomeric friction coefficient; this argument has been used to explain the behavior of the termination rate coefficient, k_t[11,12]) or by specific interactions between the ester group and the cobalt center as previously suggested by Myronichev et al.[9]

The aim of the current work is to broaden the experimental database for the CCT reaction and to further probe the influence of monomer structure. To minimize any possible interference from cobalt−carbon bond formation,[13−15] we selected *tert*-butyl methacrylate (*t*-BMA) and dimethyl itaconate (DMI) for our current studies as both monomers lead to tertiary propagating radicals. Both monomers contain bulky, and sterically demanding, side groups, and if any substituent effects other than microscopic viscosity effects are operative, we expect them to be observable in these systems. Since our primary concern is the elementary chain transfer

* Authors for correspondence. Fax: +61-2-9385 6250. E-mail: j.heuts@unsw.edu.au; t.davis@unsw.edu.au.

10.1021/ma020719m CCC: $22.00
Published on Web 12/05/2002

reaction (k_{tr}) and our measurable observable is the chain transfer constant (C_S), we need reliable k_p data. This information has recently been published for DMI, but the available k_p data for *t*-BMA are subject to some uncertainty;[16] therefore, we reinvestigated the propagation rate coefficient of *t*-BMA by pulsed-laser polymerization (PLP).

Experimental Section

Materials. *tert*-Butyl methacrylate (*t*-BMA) (Aldrich, 98%) was initially passed through a column of activated basic alumina to remove inhibitor. It was further purified by low conversion polymerization with AIBN at room temperature under UV radiation prior to vacuum distillation. Dimethyl itaconate (Aldrich 99%) was distilled under reduced pressure. The first fraction was discarded, the second was crystallized and was ground into powder. The initiators used, azobis(isobutyronitrile) (AIBN) and benzoin, were recrystallized from methanol. High purity nitrogen (BOC) was used for sparging. Benzene (Univar) was used as received. The catalytic chain transfer agent, bis[(difluoroboryl)dimethylglyoximato]cobalt(II) (COBF) was prepared according to the published method of Bakac et al.[17]

Molecular Weight Analyses. Molecular weight distributions were determined by size exclusion chromatography (SEC) using a Shimadzu LC-10 AT VP pump, a Shimadzu SIL-10AD VP Autoinjector, a column set consisting of a Polymer Laboratories 5.0 μm bead-size guard column (50 × 7.5 mm) followed by three linear PL columns (Å 10^5, 10^4, and 10^3), and a Shimadzu RID-10A differential refractive index detector. Tetrahydrofuran (BDH, HPLC grade) was used as eluent at 1 mL/min. Calibration of the SEC equipment was performed with narrow poly(methyl methacrylate) standards (Polymer Laboratories, molecular weight range: $200-1.6 \times 10^6$). The Mark−Houwink−Kuhn−Sakurada constants used were $K = 5.84 \times 10^{-5}$ dL g^{-1}, $\alpha = 0.760$ and $K = 46.5 \times 10^{-5}$ dL g^{-1}, $\alpha = 0.510$ for p(*t*-BMA)[18] and p(DMI)[19] respectively. Low concentration samples of poly(*t*-BMA) (2.5 mg/mL) and poly(DMI) (400 mg of reaction mixture/mL) were formulated in THF for analyses.

Pulsed Laser Polymerization of *t*-BMA. Monomer and initiator were charged into reaction tubes (10 mm diameter, 60 mm in height), sealed with septa and deoxygenated by sparging the solution with high purity nitrogen for 5 min. The tubes were equilibrated in a water bath at the required reaction temperature prior to laser exposure. The polymerizations were initiated by a pulsed Nd:YAG laser (Continuum Surelite I-20) with a harmonic generator (Surelite SLD-1 and SLT in series), which was used to produce the 355 nm UV laser radiation, and a wavelength separator (Surelite SSP-2), which isolates the 355 nm beam. Pulsing frequencies of 6.67, 10, and 20 Hz were used. The reaction mixtures were quenched with hydroquinone and dried to constant weight under vacuum. The conversions were kept below 5% in all experiments.

Determination of Chain Transfer Constants. A single batch of COBF, with a chain transfer constant of 28×10^3 in MMA at 60 °C, was used for all experiments described in this paper. The general procedure for the chain transfer experiments with *t*-BMA was as follows: (i) reaction times of 15 min at 60 °C and 80 min at 40 °C were used, and (ii) the AIBN concentration was kept at 0.71 mg/mL *t*-BMA with [COBF]/[*t*-BMA] between 2.39 and 8.89×10^{-7}. Since DMI has a melting point of 37−40 °C, the experimental method for DMI had to be modified as standard syringe techniques could not be used with bulk DMI. First, the initiator solution was prepared by addition of powdered DMI (15 g) and AIBN (0.025 g) to a 100 mL Schlenk flask which was subsequently sealed with a septum prior to evacuation and purging with nitrogen (repeated 5 times). Deoxygenated benzene (10 mL) was then added, and the resultant slurry was gently heated until a homogeneous solution was formed. The catalyst solution was prepared by adding COBF (1.6 mg) to a 50 mL Schlenk flask, which was subsequently evacuated and purged as described above, after which deoxygenated methanol (15 mL) was added. Five reaction ampules, modified for use with Schlenk equipment, were evacuated and purged, and catalyst solution (100−500μL) was added. These ampules were then subjected to reduced pressure to facilitate the removal of methanol, leaving behind a known amount of COBF. To each of these flasks, initiator solution (4 mL) was added. The ampules were then sealed and placed in an isothermal water bath at 60 °C for 30 min. Subsequently benzene was removed from the reaction mixtures under reduced pressure. Conversions were maintained below 6% in all experiments.

Preparation of DMI Oligomers for NMR Analysis. Powdered DMI (6 g), COBF (0.009 g) and AIBN (0.0108) were placed in a Schlenk modified reaction ampule. The flask was evacuated and flushed with nitrogen (repeated 5 times), after which it was sealed and placed in an isothermal water bath at 60 °C for 52 h. Final monomer conversion: ∼66%.

Determination of Viscosity and Density of *t*-BMA and DMI/Benzene. The viscosity of *t*-BMA monomer was determined using an A sized Ostwald viscometer immersed in an isothermal water bath. The viscometer was calibrated using known values for the density and viscosity of water. Densities of the *t*-BMA monomer and the DMI/benzene solution were determined using an Anton Paar DMA 5000 density meter. The density meter was calibrated with freshly boiled distilled water and air using known densities at 20, 40, and 60 °C. The monomer was degassed using an ultrasonic bath prior to measurement.

Matrix-Assisted Laser Desorption Ionization—Time-of-Flight (MALDI—TOF) Mass Spectrometry. MALDI analyses were either carried out using positive ion detection on a Perseptive Biosystems, Voyager DE RP instrument operated in reflectron mode or a Kratos Kompact III MALDI−TOF MS operated in linear mode. The matrix used was 2,5-dihydroxybenzoic acid (DHB, 10 mg), with NaCl (1 mg) as the cation source. The matrix and cations were dissolved in 1 mL of a methanol/water mixture (1/1 v/v). The analyte polymers were dissolved in tetrahydrofuran at a concentration of approximately 5 mg mL^{-1}. Equal parts of the matrix and polymer solution were mixed together and deposited on the target slide and stirred until dry.

Nuclear Magnetic Resonance. NMR spectra were recorded on a Bruker DMX 600 instrument with a TXI probe. The sample contained an approximately 20% solution of the DMI oligomers prepared by CCT as described above. Spectra recorded included a gradient DQF−COSY to correlate *J*-coupled protons, NOESY to correlate protons that were spatially close (<5 Å) to each other, gradient HMQC to correlate protons with directly bound ^{13}C nuclei, and gradient HMBC to correlate protons with ^{13}C nuclei two or three bonds away. All spectra were acquired in pure phase using standard procedures, the HMBC experiment being acquired with echo/antiecho phase discrimination. The proton spectral width was typically 4195 Hz. For the gradient DQF−COSY, 512 × 4096 points were collected with 2 scans per increment, an acquisition time of 488 ms, and a recycle delay of 7 s. Parameters for the NOESY were as per the COSY except with 8 scans per increment and the mixing time was 600 ms. The gradient HMQC was acquired with 1024 × 2048 points and 2 scans per increment, an acquisition time of 244 ms and a recycle delay of 2 s. The F_1 spectral width was 22637 Hz. The gradient HMBC was acquired with 1024 × 4096 points and 2 scans per increment, an acquisition time of 244 ms and a recycle delay of 2 s. The F_1 spectral width was 22637 Hz. Spectra were zero filled by a factor of 2 in F_2 and four in F_1 before processing. 90° shifted squared-sine bell apodization functions were applied in both dimensions of spectra except for F_2 or the HMBC where it was shifted 60°. Chemical shifts are relative to residual $CHCl_3$ set to 7.26 ppm for ^{1}H and relative to $CDCl_3$ set to 77.0 ppm for ^{13}C. Assignments are as follows (see Figures 8 and 9).

Species **A**. ^{1}H NMR: 6.776 (s), alkene; 3.13, 3.20 (CH_2, AB, $J = 13$ Hz); 2.79, 2.39 (CH_2, AB, $J = 16.9$ Hz); 1.221 (s), CH_3. ^{13}C NMR: 175.1, 171.5, 165.8, 167.4, 143.8, 129.0 (CH), 44.4, 41.8 (CH_2), 35.2 (CH_2), 21.8 (CH_3).

Species **B**. ^{1}H NMR: 6.728 (s), alkene; 3.35, 3.30 (CH_2, AB, $J \sim 13.0$ Hz); 2.79, 2.28 (CH_2, AB, $J = 15.8$ Hz); 2.78, 2.71 (CH_2, AB, $J \sim 17$ Hz); 2.49, 2.06 (CH_2, AB, $J = 14.9$ Hz); 1.131 (s), CH_3. ^{13}C NMR: 176.3, 174.4, 171.1, 165.7, 167.3, 143.1, 129.0 (CH), 47.9, 43.6, 45.5 (CH_2), 36.9 (CH_2), 43.4 (CH_2), 34.2 (CH_2), 20.7 (CH_3).

Species **C**. ^{1}H NMR: 6.715 (q, $J = 1.6$ Hz), alkene; 2.225 (d, $J \sim 1.6$ Hz), CH_3. ^{13}C NMR: 167.5, 166.3, 143.6, 127.4 (CH), 14.5 (CH_3).

Species **D** (partial only). ^{1}H NMR: 6.712 (s), alkene; 3.36, 3.24 (CH_2, AB, $J = 13.2$ Hz); 1.297 (s), CH_3. ^{13}C NMR: 167.6, 165.8, 143.8, 129.1 (CH), 33.7 (CH_2), 22.5 (CH_3).

Species **E**. ^{1}H NMR: 6.626 (q, $J = 1.7$ Hz), alkene; 2.225 (d, $J = 1.7$ Hz), CH_3; ^{13}C NMR: 166.2, 164.0, 149.3, 129.7 (CH), 11.3 (CH_3).

Species **F** (partial only). ^{1}H NMR: 5.855 (t, $J \sim 1.0$ Hz), alkene; 2.77, 2.72 (CH_2, AB, $J \sim 14$ Hz); 1.221 (s), CH_3. ^{13}C NMR: 168.6, 164.9, 144.8, 125.0 (CH), 44.1, 41.6 (CH_2), 22.5 (CH_3).

Species **G** (partial only). ^{1}H NMR: 5.802 (q, $J = 1.7$ Hz), alkene; 1.999 (d, $J = 1.7$ Hz), CH_3; ^{13}C NMR: 169.4, 145.8, 120.6 (CH), 20.7 (CH_3).

Species **H** (partial only). ^{1}H NMR: 5.773 (t, $J \sim 1.0$ Hz), alkene; 3.02, 2.89 (CH_2, AB, $J \sim 13.0$ Hz); 2.73, 2.28 (CH_2, AB, $J \sim 16$ Hz); 2.37, 1.99 (CH_2, AB, $J = 14.5$ Hz); 1.118 (s), CH_3. ^{13}C NMR: 174.1, 168.8, 145.0, 124.8 (CH), 43.6, 45.1 (CH_2), 41.6 (CH_2), 43.4 (CH_2), 34.2 (CH_2), 20.3 (CH_3).

The methoxy resonances were not assigned due to a high degree of overlap, but there are resonances in appropriate places for all species listed in Figure 9.

Results and Discussion

1. Catalytic Chain Transfer Polymerization of *t*-BMA. The catalytic chain transfer behavior of *t*-BMA was studied in an attempt to distinguish possible substituent and viscosity effects on the chain transfer rate. As a reference system we can use *n*-BMA, which has a viscosity similar to that of *t*-BMA (vide infra), but a less sterically demanding ester group. If interactions between the substituent and the cobalt center are important, then a decrease in the k_{tr} for the *t*-BMA system can be expected.

(a) Viscosity and Density Measurements. The density of *t*-BMA was measured using an Anton Paar DMA 5000 density meter in the temperature range 22−60°C and was found to adhere to the relation

$$\rho = 1.1748 - 1.014 \times 10^{-3} T \qquad (2)$$

where ρ is the density in g cm^{-3} and T is the temperature in K. The viscosity of *t*-BMA was determined using an Ostwald viscometer at 60 °C and was found to be 0.53 cP.

(b) Propagation Rate Coefficient of *t*-BMA. Since the only experimentally accessible kinetic parameter for chain transfer is the chain transfer constant, C_S, and we wish to study directly the chain transfer rate coefficient, k_{tr}, it is necessary to have information about the propagation rate coefficient of *t*-BMA. Although propagation rate coefficients for *t*-BMA have been reported previously,[16] the results are subject to uncertainty; the reported Arrhenius parameters do not appear to follow general trends observed in the methacrylate series of monomers.[20,21] Since this work preceded the consistency checks that are now realized to be essential for reliable PLP data, a reassessment of *t*-BMA propagation data is desired. We therefore measured the propagation rate coefficient of *t*-BMA using PLP in the temperature range 22−60 °C.

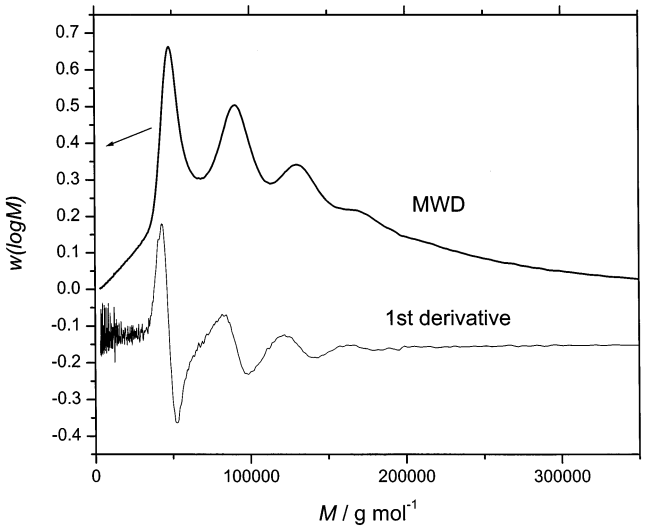

Figure 1. Typical molecular weight distribution generated in a pulsed-laser experiment of *t*-BMA at 40 °C using benzoin as initiator and a pulsing frequency of 10 Hz.

Table 1. Experimental PLP Data for *t*-BMA

temp (°C)	init[a]	[M] (mol L^{-1})	[I] (mg mL^{-1})	pulsing freq (Hz)	first inflectn (amu)	second inflectn (amu)	k_p (dm^3 mol^{-1} s^{-1})
22	A	6.16	1.61	10.00	26 250	51 218	300
22	A	6.16	0.97	10.00	26 413	51 246	302
22	A	6.16	0.94	6.67	38 483	74 629	293
22	B	6.16	1.07	10.00	27 052	52 064	309
30	A	6.10	1.11	10.00	32 817	63 577	378
30	A	6.10	1.92	10.00	32 846	63 187	379
30	A	6.10	1.18	6.67	48 651	48 651	374
30	B	6.10	0.98	10.00	33 568	63 964	387
40	A	6.03	0.77	10.00	42 842	82 339	500
40	A	6.03	0.88	6.67	62 557	121 494	486
40	A	6.03	1.75	20.00	22 431	43 336	523
40	A	6.03	1.26	10.00	42 850	82 675	500
40	B	6.03	1.15	10.00	43 242	83 228	504
50	A	5.96	1.32	10.00	54 436	105 178	643
50	A	5.96	1.00	20.00	28 689	54 981	677
50	A	5.96	1.55	10.00	53 969	106 468	637
50	B	5.96	1.23	10.00	53 825	106 212	635
60	A	5.89	1.63	20.00	35 764	68 643	855
60	A	5.89	0.90	10.00	67 634	130 857	808
60	A	5.89	1.00	20.00	36 181	68 337	865
60	B	5.89	1.71	20.00	35 171	66 161	840

[a] Initiator: A = AIBN; B = benzoin.

A typical molecular weight distribution obtained from a PLP experiment is shown in Figure 1. Inflection points were found to be independent of initiator type and concentration, overtones are observed at multiples of the primary peak, and k_p was found to be independent of pulsing rate. Thus, the consistency checks recommended by an IUPAC working party[20−22] have been satisfied. A summary of the PLP results are shown in Table 1, where it should be noted that k_p was determined from the first inflection point. Figure 2 shows the Arrhenius plot of the data presented in Table 1, and yields an activation energy, E_a, of 22.1 kJ mol^{-1} with a preexponential factor, A, of 2.4×10^6 dm^3 mol^{-1} s^{-1}. If we compare these Arrhenius parameters with those of *n*-BMA[20] and *i*-BMA[23] (see Table 2), it can be seen that all three monomers have comparable activation energies (as expected from the similar electronic nature of the monomers). The preexponential factor for *t*-BMA, however, is around 80% of the value found for *i*-BMA and about 66% of that for *n*-BMA; this observation is

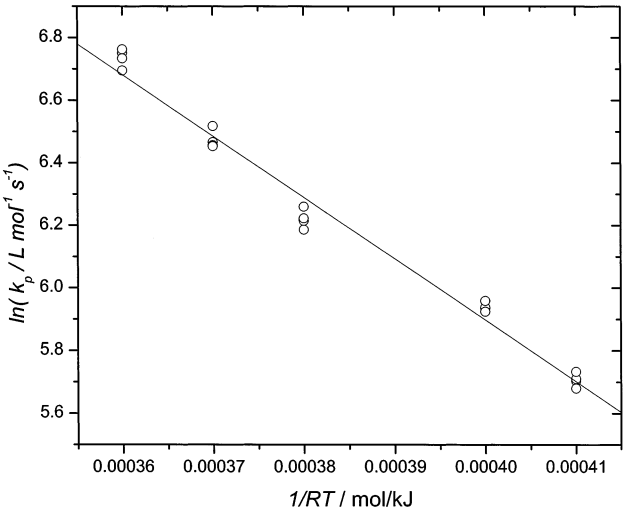

Figure 2. Arrhenius plot of the propagation rate coefficient of *t*-BMA.

Table 2. Experimental PLP Data for *n*-, *i*-, and *t*-BMA

				k_p (L mol^{-1} s^{-1})	
monomer	solvent	A (L mol^{-1} s^{-1})	E_a (kJ/mol)	40 °C	60 °C
n-BMA[20]	bulk	3.80×10^6	22.9	576	976
i-BMA[23]	bulk	3.17×10^6	22.5	564	947
t-BMA[a]	bulk	2.40×10^6	22.1	503	836
t-BMA[16]	bulk	2.51×10^7	27.7	601	1140

[a] This work.

Table 3. Chain Transfer Constants of *t*-BMA at 40 and 60 °C

temp (°C)	C_S[a]	C_S[b]	convn (%)
40	16.3×10^3	18.6×10^3	1.9−1.3
40	13.7×10^3	14.2×10^3	1.8−1.0
40	11.1×10^3	13.6×10^3	1.9−1.0
40	13.8×10^3	15.5×10^3	1.8−0.7
40	13.7×10^3 [c]	15.5×10^3 [c]	
60	13.3×10^3	14.7×10^3	3.4−2.6
60	13.3×10^3	14.0×10^3	3.4−2.7
60	15.0×10^3	16.8×10^3	3.3−2.5
60	14.6×10^3	15.9×10^3	3.3−2.5
60	14.3×10^3	13.9×10^3	3.2−2.5
60	14.1×10^3 [d]	15.1×10^3 [d]	

[a] Chain transfer constant determined using the Mayo method based on M_n. [b] Chain transfer constant determined using the Mayo method based on $M_w/2$. [c] Average value at 40 °C. [d] Average value at 60 °C.

consistent with an increased steric hindrance caused by the bulky ester group.

(c) Chain Transfer Constant Determination of *t*-BMA. A total of nine experiments, each of four different catalyst:monomer ratios, were carried out, five at 60 °C and four at 40 °C; these data are presented in Table 3. Typical molecular weight distributions obtained are shown in Figure 3. All molecular weight distributions show polydispersity indices of around 2, consistent with a chain transfer dominated chain stopping mechanism and conversion also decreases with increasing concentration of COBF, consistent with earlier observations in CCT studies.[24,25] The chain transfer constant was determined by the Mayo method (Figure 4) and has a value of about 15×10^3 at 60 °C, i.e., about 50% of that in MMA. In Table 4, the values for the product $C_S k_p \eta_{monomer}$ for *t*-BMA, *n*-BMA, and MMA are compared; it should be noted that there are minor variations to the numbers quoted previously,[2] because values of

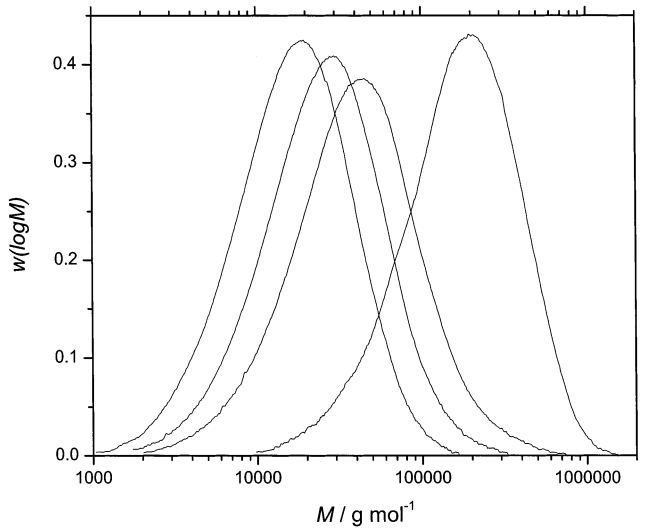

Figure 3. Molecular weight distributions of a typical C_S experiment of COBF with *t*-BMA (60 °C, [COBF]/[*t*-BMA] = $(2.39-8.89) \times 10^{-7}$)

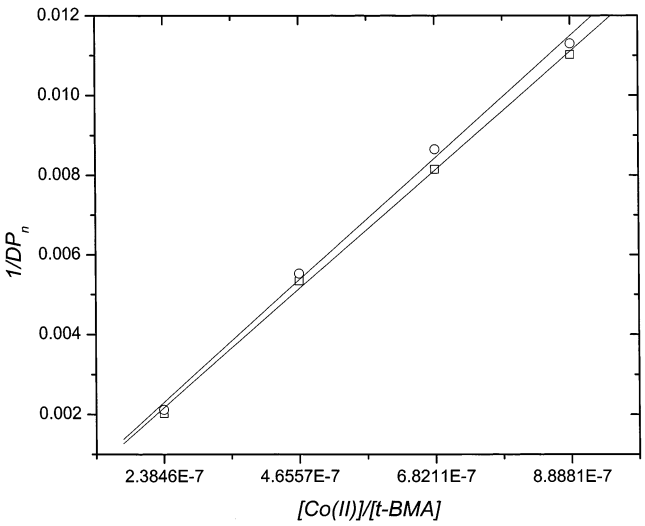

Figure 4. Mayo plot from the molecular distributions shown in Figure 3 ((○) based on $M_w/2$; (□) based on M_n).

Table 4. Relationship between Viscosity and Chain Transfer Constant

monomer	temp (°C)	C_S[a]	viscosity (cP)	k_p (L mol^{-1} s^{-1})	$C_S k_p \eta$
t-BMA	60	15.1×10^3	0.53	836	6.7×10^6
n-BMA	60	16.1×10^3	0.55	976	8.6×10^6
MMA	60	28.1×10^3	0.37	833	8.6×10^6

[a] Chain transfer constant based on $M_w/2$.

k_p have been adjusted to those given by an IUPAC recommendation.[20] It is clear from the data in Table 4 that the product $C_S k_p \eta_{monomer}$ for *t*-BMA is lower than the other two values. Considering the scatter in the used chain transfer constants this variation lies on the borderline of significance. On one hand, the result may indicate that the relationship between monomer viscosity and chain transfer constant is more complex and deviations become more evident when the molecular structure is altered ($C_S \approx 19 \times 10^3$ for *t*-BMA is required to give the same product as for *n*-BMA and MMA; this high value for C_S appears to be outside the experimental range). On the other hand, the 20% reduction in k_{tr} for *t*-BMA as compared to that of *n*-BMA is consistent with

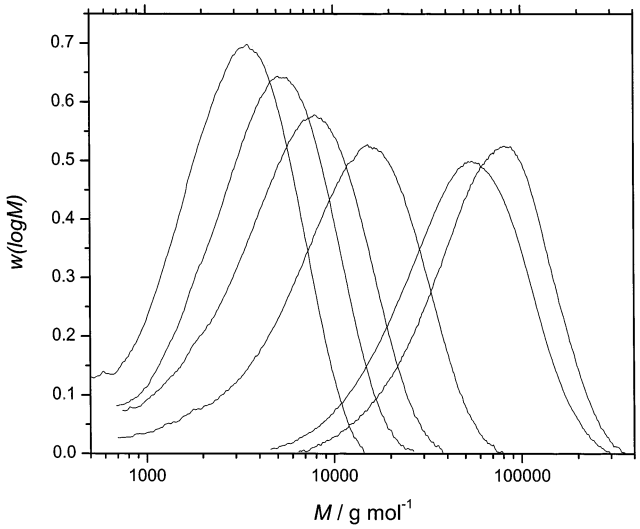

Figure 5. Molecular weight distributions of a C_S determination experiment of DMI with COBF (60 °C, [COBF]/[DMI] = 0, 2.06×10^{-6} to 1.04×10^{-5})

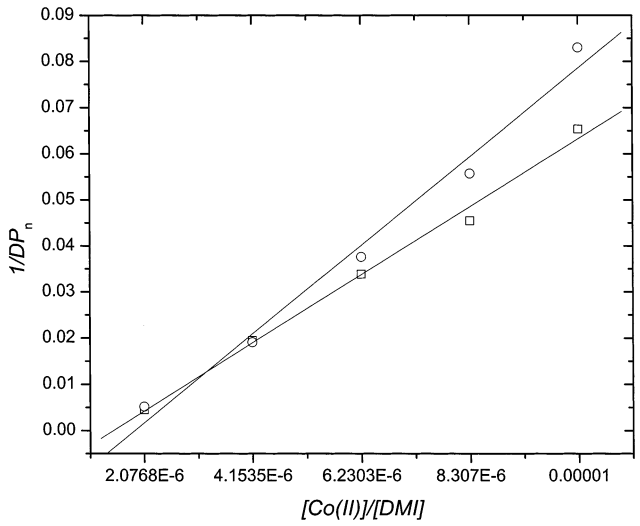

Figure 6. Mayo plot for the C_S determination of DMI with COBF (60 °C, [COBF]/[DMI] = 2.06×10^{-6} to 1.04×10^{-5}).

a more hindered transition state for the H-abstraction reaction. The steric hindrance results in a frequency factor for *t*-BMA propagation which is about 66% of that in *n*-BMA, and if the involved transition state in the current hydrogen abstraction is similar to that previously studied in organic radical systems, then similar steric substituent effects in H-transfer and propagation are expected, with a slightly smaller effect in the H-transfer reaction.[26] However, at this point, we feel that both arguments are too speculative to dismiss either of the two proposed mechanisms.

Table 5. MALDI−TOF Assignments of DMI Oligomers

species	mass (exptl)	mass (theor)
$(DMI)_5Na^+$	813.12	813.98
$(DMI)_6Na^+$	971.76	972.18
$(DMI)_7Na^+$	1130.00	1130.38
$I-(DMI)_5Na^+$	not observed	880.98
$I-(DMI)_6Na^+$	not observed	1039.18
$I-(DMI)_7Na^+$	not observed	1197.38

2. Catalytic Chain Transfer Polymerization of Dimethyl Itaconate. In an attempt to enhance any possible interactions between the substituents in the radical and the cobalt catalyst we studied the highly hindered monomer DMI. This monomer was found to have both a low k_p,[19] attributed to a low value for *A* caused by steric hindrance and a very low value for the termination rate coefficient k_t of about 10^5 dm^3 mol^{-1} s^{-1}, which displays a virtually chain-length independent behavior.[27] The latter observation is in clear contrast with the behavior of k_t in common monomers such as MMA, where termination is diffusion-controlled and k_t shows a chain-length dependence.[12,28] Irrespective of the exact nature of the reduced k_t in DMI polymerization, it is clear that the large substituents affect the dynamics of the termination reaction, and it is therefore conceivable that similar effects may be operative in the hydrogen abstraction reaction. Since there should be no interference from cobalt−carbon bond formation, this system is ideal for the study of substituent effects.

(a) Viscosity and Density Measurements. The density of the DMI/benzene (1.72:1 w/w) solution, used in chain transfer constant measurements, was determined to be 1.015 g mL^{-1} at 22 °C. The viscosity of DMI at 60 °C was estimated using an Ostwald viscometer. We were unable to measure the viscosity accurately as the DMI started to polymerize during the measurements. As an upper limit of the viscosity at 60 °C we found a value of 1.62 cP.

(b) Chain Transfer Constant Determination of DMI. The chain transfer constant of DMI in benzene

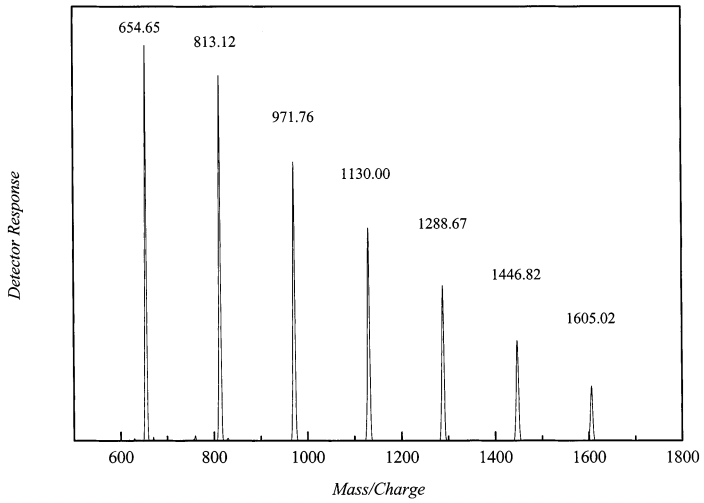

Figure 7. MALDI−TOF spectrum of DMI oligomers (DHB/NaCl matrix).

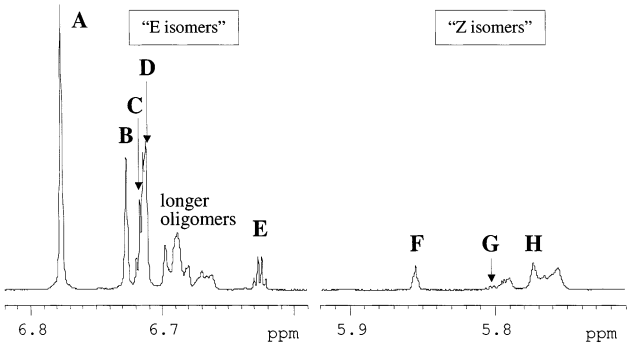

Figure 8. 600 MHz ^{1}H NMR spectrum of the alkene region of DMI oligomers prepared by CCT. Used solvent is $CDCl_3$. Peak labels correspond to the structures shown in Figure 9.

at 60 °C was determined via the Mayo equation to be 7.3×10^3 from M_n data and 9.5×10^3 from $M_w/2$ data (two experiments); molecular weight distributions and Mayo plots of these experiments are shown in Figures 5 and 6, respectively. From the chain transfer constant, a value of about 2.6×10^5 dm^3 mol^{-1} s^{-1} is obtained for k_{tr}, which is around 2 orders of magnitude lower than for MMA with COBF at 60 °C. If this decrease were only caused by a simple (monomer) viscosity effect, the DMI viscosity would have to be 2 orders of magnitude higher than that of MMA, which is clearly not the case ($\eta_{monomer} < 1.62$ cP, vide supra). Furthermore, since DMI forms a highly hindered tertiary radical, the formation of carbon−cobalt bonds, with an accompanying decrease in C_S, is virtually impossible.[5] Hence the low value for C_S (and k_{tr}) is conceivably caused by steric hindrance arising from the large substituents on the radical. This hindrance may be a direct interaction between the radical substituents and the cobalt center[9] or may reduce the segmental mobility within the radical causing a reduction in the segmental diffusion rate.[6]

(c) Mechanistic Aspects. To further investigate the low C_S for DMI and whether the chain transfer process is similar to that in the methacrylates, we studied the

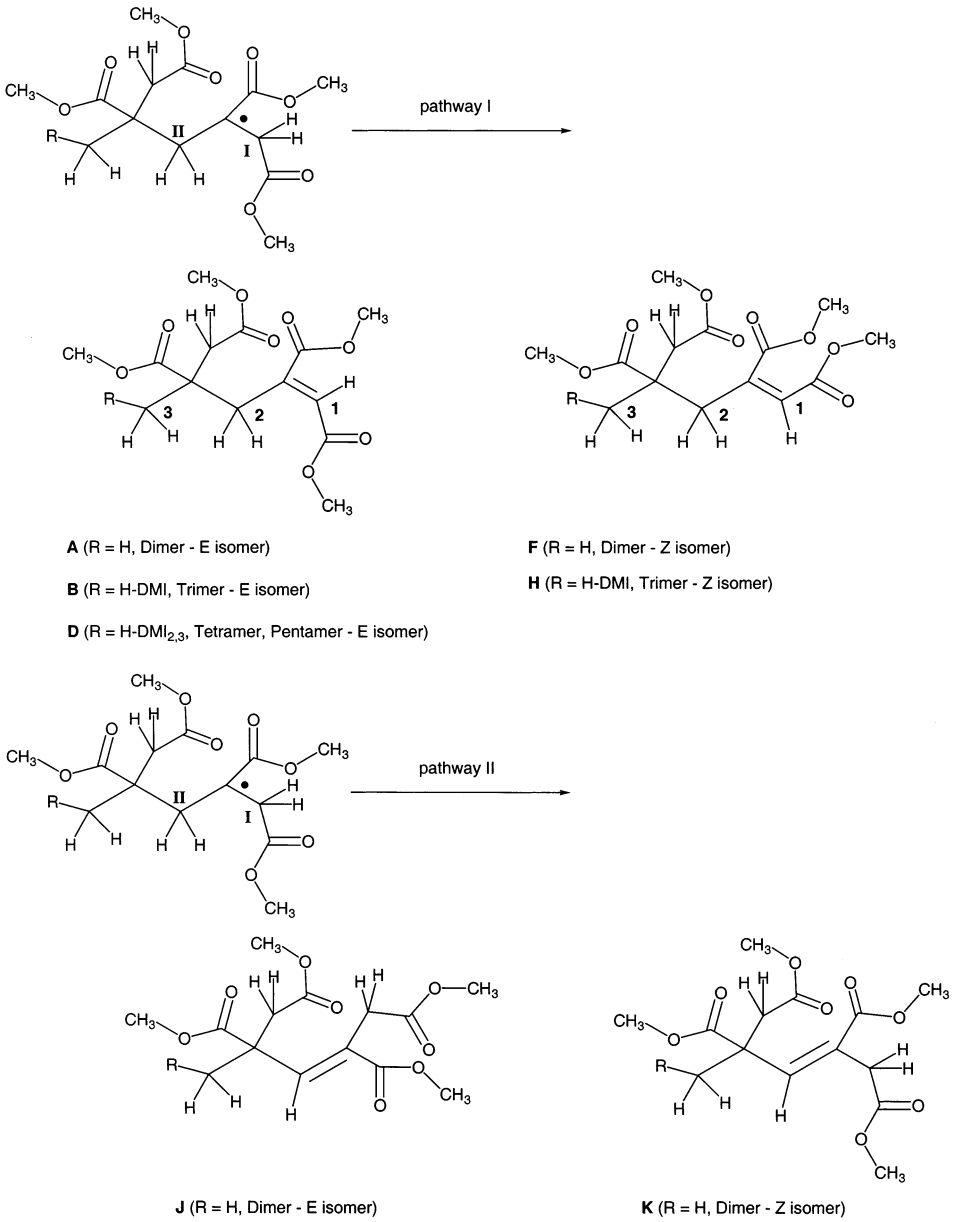

Figure 9. Possible chain transfer paths for DMI macroradical with COBF: (a) pathway I corresponds to hydrogen abstraction from the α-substituent; (b) pathway II corresponds to hydrogen abstraction from the polymer backbone. The oligomeric species shown correspond to possible structures in the NMR spectra of the oligomers studied.

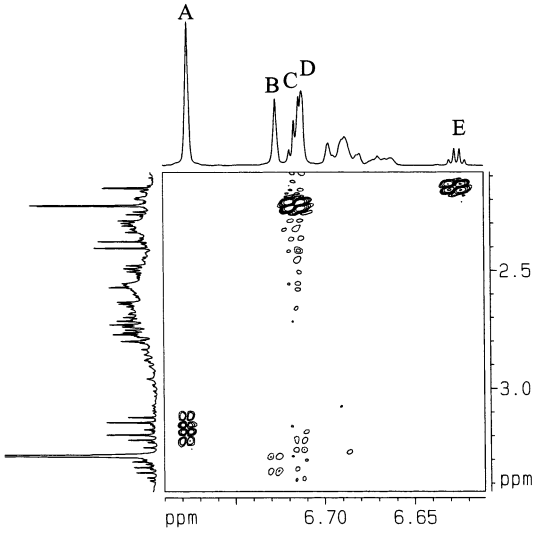

Figure 10. Expanded region of the DQF−COSY spectrum of DMI oligomers showing correlations between alkene and aliphatic protons. Annotated with normal ^{1}H NMR spectra along each axis.

structures of oligomeric DMI molecules produced via CCT (see Experimental Section) using MALDI−TOF and NMR analysis. The number-average molecular weight of the studied oligomers was determined by SEC (M_n = 536), ^{1}H NMR (M_n = 623) and MALDI−TOF (M_n = 824; see Figure 7). The observed differences are caused by the fact that all three methods employed had an inherent flaw: (1) SEC is expected to give inaccurate results as the refractive index is not independent of molecular weight for these low molecular weight polymers;[29] (2) NMR, where M_n was obtained by using the ratio of methonate (3.5−3.8 ppm) protons to the vinylic proton (6.7−6.9 ppm), yields an underestimate for M_n, because monomer could not be effectively removed from the oligomers (the polymer is too low in molecular weight to be precipitated, while the monomer has too high a boiling point for evaporation); (3) MALDI−TOF gives an overestimation as the dimer peak was not included in the calculation of M_n. Overall we can state that the average chain length of the prepared oligomers is about 4−5.

Figures 7 and 8 show that the same CCT process is operative with DMI as with previously studied monomers. The ^{1}H NMR spectrum (Figure 8) shows the existence of vinylic protons, indicating that chain growth is stopped via the abstraction of a hydrogen atom. Multiple vinyl peaks are observed between 6.7 and 6.9 ppm, which correspond to dimer (6.9 ppm), trimer (6.75 ppm), and larger unresolved oligomers (6.7 ppm). The reasonable agreement between the values of M_n obtained by MALDI, NMR and GPC is a further indication that all chains contain a vinyl end group. Proof of initiation by hydrogen atoms (i.e., the second characteristic of the "traditional" CTT mechanism[30,31]) is provided by the MALDI spectrum of the oligomers. Figure 8 clearly shows that all peaks correspond to oligomers initiated by hydrogen and that the series of peaks corresponding to initiation by AIBN fragments are absent (Table 5).

A further interesting aspect of the CCTP of DMI is the position of the vinyl group in the chain end. It is a well-known fact that the abstracted hydrogen in the CCTP of methacrylates originates from the α-methyl group of the terminal unit in the radical, whereas a

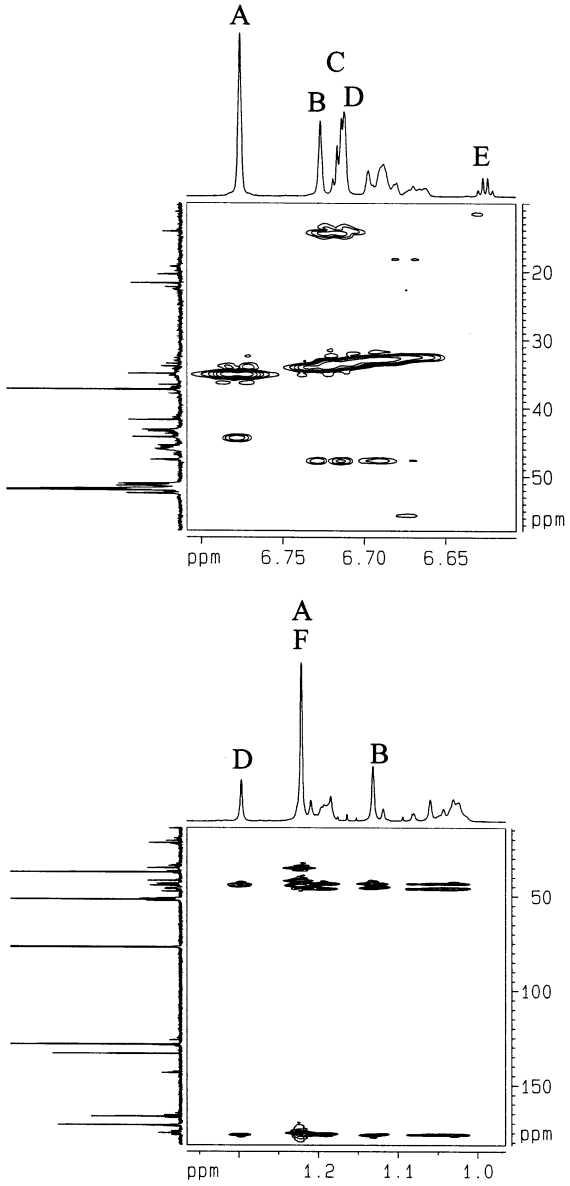

Figure 11. Expansions of the HMBC spectrum of DMI oligomers, showing (above) cross-peaks between alkene protons and aliphatic carbons (note lack of correlation to a methyl carbon for proton labeled A for example) and (below) cross-peaks between methyl protons and all carbons (note general lack of correlations to any alkene carbons in the 100−150 ppm region). Spectrum is annotated with normal ^{1}H (F_2) and ^{13}C NMR (F_1) spectra.

hydrogen is abstracted from the β-carbon in the backbone of the propagating radical in the case of styrene.[30,31] It is not a priori clear where hydrogen abstraction would occur in a propagating DMI-derived radical, as two sterically hindered methylene groups are present in the β-position to the radical. The two possible routes of hydrogen abstraction are shown in Figure 9. It is clear that hydrogen abstraction from C^I is less hindered than from C^{II}, but it is still quite hindered. Furthermore, possible electronic effects are likely to be different: C^{II} has a carbon-centered radical in its α position and two carbonyl groups in a β position, whereas C^I has a carbon-centered radical and a carbonyl group in an α position and another carbonyl group in a β position.

(d) NMR Studies of the CCT Pathway in DMI. NMR studies were performed to identify the nature of the vinyl group in the DMI oligomers. The regions of

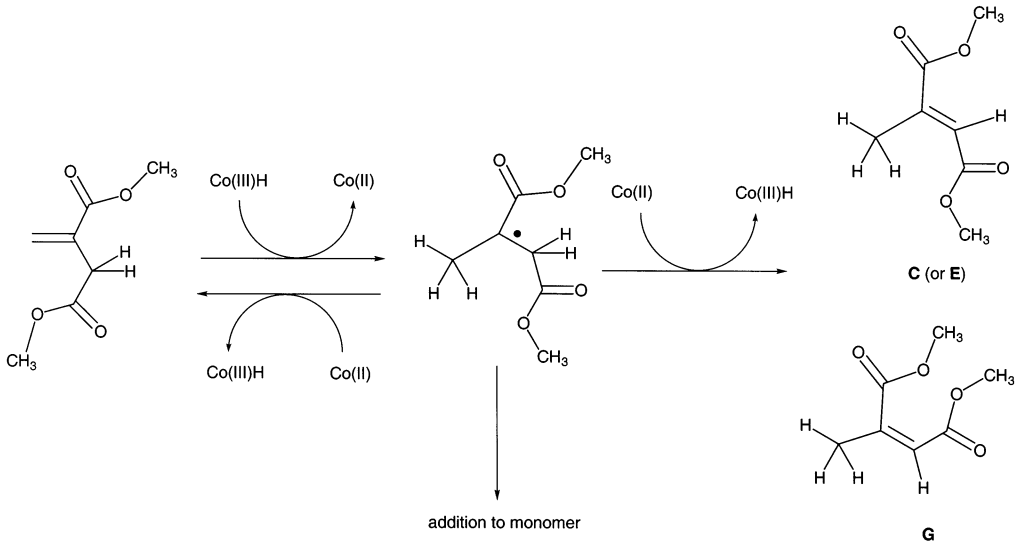

Figure 12. Catalytic chain transfer process involving a monomeric radical resulting in the formation of dimethyl mesaconate (**C**) and dimethyl citraconate (**G**).

the ^{1}H NMR spectra attributable to alkene protons produced by the hydrogen abstraction from the growing radicals is shown in Figure 8. The two regions of resonances have been labeled "*E* isomers" and "*Z* isomers" reflecting the stereochemistry of the ester functions (−CO_2Me) attached to the alkene moiety. The assignments made in Figure 9 are obtained from detailed analysis of the 2D NMR spectra. The key question to answer was at which carbon in the terminal unit of the oligomer/polymer did hydrogen abstraction occur? There are two possibilities which, in the case of a dimer, can lead to species of types **A** and **F** (both observed—from pathway I) or types **J** and **K** (not identified in the mixture—from pathway II). For example, species **A** is assigned fully starting from the alkene proton at 6.776 ppm and attached carbon at 129.0 ppm (labeled **1**). Although an apparent singlet, this resonance shows clear cross-peaks in the COSY spectrum (see Figure 10) to protons at 3.132 and 3.206 ppm which are attached to a carbon at 35.2 ppm (labeled **2**) suggesting the protons of types **1** and **2** are separated by four bonds. In the HMBC spectrum (see Figure 11), proton **1** shows clear cross-peaks to carbon **2** as well as the carbonyl carbons attached to the double bond, but, significantly, no correlation to the aliphatic methyl carbon (labeled **3**). Similarly, the aliphatic methyl protons (**3**) do not correlate to any alkene carbons, but only to those carbons within three bonds as expected. The methylene protons labeled **2**, and indeed all protons within **A**, show correlations to every carbon within three bonds. That **A** is the *E* isomer is apparent from three pieces of data: (i) the NOESY spectrum shows only a very small NOE (<0.5%) between protons labeled **1** and **2**; (ii) the couplings through two and three bonds between the alkene proton and both of the carbonyl carbons attached to the double bond are small (<6 Hz) implying neither of them is trans to the alkene proton; (iii) the chemical shift is consistent with this *E* stereochemistry.

Although a complete assignment of protons and carbons in compound **F** was not possible due to overlap and low intensity of cross-peaks, the pattern of cross-peaks in the HMBC spectrum involving the groups labeled **1**, **2**, and **3** mirrors that observed in compound **A** suggesting that it is the opposite isomer. That **F** is the *Z* isomer is confirmed by the following facts: (i) the NOESY spectrum shows a sizable NOE (ca. 3.2%) between protons labeled **1** and **2**; (ii) the coupling between the alkene proton and one of the carbonyl carbons attached to the double bond (168.6 ppm) is large (ca. 11 Hz), implying this carbonyl is trans to the alkene proton; (iii) the chemical shift is consistent with this *Z* stereochemistry.

The key to identifying structures of types **J** and **K**, arising from reaction pathway II, would be in the HMBC spectra, where a cross-peak from an aliphatic methyl group to the protonated alkene carbon would be observed along with a correlation from the alkene proton to the aliphatic methyl carbon. No species generating this distinctive pattern could be clearly identified suggesting the amount of these compounds is nil or very small. A small amount of **J** and **K** may be present, for example, a low intensity, highly overlapped alkene proton peak at 6.673 ppm shows a correlation to a methyl group in the HMBC spectrum; this may be consistent with structure **J**, but could not be clearly assigned. The preference for the hydrogen-abstraction reaction leading to structures of types **A** and **F** (pathway I) over types **J** and **K** (pathway II) is clear and a conservative estimate would place at least a factor of 10 preference and possibly very much more than this amount.

Compounds **C** and **G** (see Figure 12) have been identified as dimethyl mesaconate and dimethyl citraconate, respectively. Deriving the structure from the NMR data is straightforward and the values obtained agree well with literature data.[32,33] These two molecules are produced from a hydrogen-abstraction reaction involving a monomeric DMI radical. From the low observed polymerization rate (only ∼66% conversion after 52 h) and relatively small amounts of **C** and **G**, it can be concluded that the hydrogen abstraction leading to **C** and/or **G** is much slower than the hydrogen abstraction from the α-methyl group which results in the formation of monomer. The presence of compounds **C** and **G** is interesting as a hydrogen-transfer reaction to these compounds potentially leads to a secondary radical, which could undergo a Co−C bond formation reaction and hence lead to (reversible) catalyst deactivation. However, it is unlikely that this process plays a

significant role as both vinyl compounds are very sterically hindered, making a hydrogen transfer reaction unlikely and any possible hydrogen transfer would most likely occur to the least hindered carbon atom, which would then result in a tertiary radical rather than a secondary radical. Finally, it should be noted that species **E** gives a pattern almost identical to that for **C** in the HMBC and is clearly very similar. It is unclear what the difference is at this point.

In a fashion similar to that outlined for **A** and **F**, detailed analysis of the NMR data shows that species **B**, **D**, and **H** are consistent with being the trimer with E, tetramer with E and trimer with Z stereochemistry, respectively. Resonances for **B** were fully assigned but only partially assigned for **D** and **H**.

Integration of the entire "*E* isomer" region vs the entire "*Z* isomer" region gives a relative intensity of 5.1:1. Integration of the E/Z pair consisting of compounds **A** and **F** gives a ratio of 9.34:1. Overall, the present NMR study suggests that the hydrogen-abstraction reaction proceeds via pathway I and favors production of the *E* isomer over the *Z* isomer by a factor of between 5 and 10:1.

In summary, it can be concluded that the hydrogen abstraction step in the CCTP of DMI involves the hydrogens in the α-substituent of the radical rather than backbone hydrogens and that the product contains predominantly *E* isomers.

Conclusions

In this study, we attempted to clarify the role of monomer substituent effects in catalytic chain transfer polymerization by using two hindered monomers, in which steric hindrance would potentially lower the chain transfer rate coefficient further than that expected from monomer viscosity effects. *t*-BMA displayed behavior very similar to other methacrylates, in that the approximate relationship given by eq 1 provided a reasonable description for this system. However, the difference between the observed chain transfer rate coefficient and that expected from simple viscosity arguments borders on being significant and may indicate that direct steric hindrance in the hydrogen-abstraction reaction plays a role.

The results obtained for the CCTP of DMI allow for a less speculative discussion. It was found that DMI undergoes a similar CCTP as compared to the methacrylates, i.e., the abstraction of a hydrogen atom from the α-substituent (with an overwhelming preference to form the *E* isomer) followed by hydrogen initiation of a monomer molecule. High chain transfer constants are observed, but the resulting value for k_{tr} is about 2 orders of magnitude lower than that for MMA under similar conditions. This value cannot be explained in terms of our postulated relationship between k_{tr} and the monomer viscosity (eq 1) and thus suggests a more pronounced substituent effect. As yet it is not clear whether this effect is caused by a direct interaction between radical substituent and the cobalt center or whether the large substituents lead to a stiffer polymer chain and a corresponding reduced segmental diffusion rate.

Acknowledgment. Useful discussions regarding the propagation rate coefficient of *t*-BMA with Professor Bob Gilbert, useful comments by Dr Steven Ittel, the award of an Australian Postgraduate Award to G.E.R., and financial support by ICI Plc. and the Australian Research Council are all gratefully acknowledged.

References and Notes

(1) For general reviews on catalytic chain transfer polymerization, see: (a) Karmilova, L. V.; Ponomarev, G. V.; Smirnov, B. R.; Bel'govskii, I. M. *Russ. Chem. Rev.* **1984**, *53*, 132. (b) Davis, T. P.; Haddleton, D. M.; Richards, S. N. *J. Macromol. Sci., Rev. Macromol. Chem. Phys.* **1994**, *C34*, 243. (c) Davis, T. P.; Kukulj, D.; Haddleton, D. M.; Maloney, D. R. *Trends Polym. Sci.* **1995**, *3*, 365. (d) Gridnev, A. *J. Polym. Sci., Polym. Chem.* **2000**, *38*, 1753. (e) Gridnev, A. A.; Ittel, S. D. *Chem. Rev.* **2001**, *101*, 3611. (f) Heuts, J. P. A.; Roberts, G. E.; Biasutti, J. D. *Aust. J. Chem.* **2002**, *55*, 381.

(2) Heuts, J. P. A.; Forster, D. J.; Davis, T. P. *Macromolecules* **1999**, *32*, 3907.

(3) Forster, D. J.; Heuts, J. P. A.; Davis, T. P. *Polymer* **1999**, *41*, 1385.

(4) Forster, D. J.; Heuts, J. P. A.; Lucien, F. P.; Davis, T. P. *Macromolecules* **1999**, *32*, 5514.

(5) Heuts, J. P. A.; Forster, D. J.; Davis, T. P. In *Transition Metal Catalysis in Macromolecular Design*; Boffa, L. S., Novak, B. M., Ed.; ACS Symposium Series 760; American Chemical Society: Washington, DC, 2000; p 254.

(6) Roberts, G. E.; Davis, T. P.; Heuts, J. P. A.; Russell, G. T. *J. Polym. Sci., Polym. Chem.* **2002**, *40*, 782.

(7) See, for example: (a) Barner-Kowollik, C.; Vana, P.; Davis, T. P. In *Handbook of Radical Polymerization*; Matyjaszewski, K.; Davis, T. P.; Eds.; Wiley-Interscience: New York, 2002; p 1. (b) Moad, G.; Solomon, D. H. *The Chemistry of Free Radical Polymerization*; Pergamon: Oxford, England, 1995. (c) O'Driscoll, K. F. In *Comprehensive Polymer Science*; Eastmond, G. C., Ledwith, A., Russo, S., Sigwalt, P., Ed.; Pergamon Press: Oxford, England, 1989; Vol. 3, p 161.

(8) Haddleton, D. M.; Maloney, D. R.; Suddaby, K. G.; Muir, A. V. G.; Richards, S. N. *Macromol. Symp.* **1996**, *111*, 37.

(9) Mironychev, V. Y.; Mogilevich, M. M.; Smirnov, B. R.; Shapiro, Y. Y.; Golikov, I. V. *Polym. Sci. USSR* **1986**, *28*, 2103.

(10) Pierik, S. C. J. Shining a Light on Catalytic Chain Transfer Ph.D. Thesis, Technische Universiteit Eindhoven, 2002.

(11) Mahabadi, H. K.; O'Driscoll, K. F. *J. Polym. Sci., Polym. Chem.* **1977**, *15*, 283.

(12) O'Driscoll, K. F. In *Comprehensive Polymer Science*; Eastmond, G. C., Ledwith, A., Russo, S., Sigwalt, P., Ed.; Pergamon Press: Oxford, England, 1989; Vol. 3, p 161.

(13) Roberts, G. E.; Heuts, J. P. A.; Davis, T. P. *Macromolecules* **2000**, *33*, 7765.

(14) Heuts, J. P. A.; Forster, D. J.; Davis, T. P.; Yamada, B.; Yamazoe, H.; Azukizawa, M. *Macromolecules* **1999**, *32*, 2511.

(15) Gridnev, A. A.; Belgovskii, I. M.; Enikolopyan, N. S. *Dokl. Akad. Nauk SSSR* (*Engl. Transl.*) **1986**, *289*, 1408.

(16) Pascal, P.; Winnik, M. A.; Napper, D. H.; Gilbert, R. G. *Makromol. Chem. Rapid Commun.* **1993**, *14*, 213.

(17) Bakac, A.; Brynildson, M. E.; Espenson, J. H. *Inorg. Chem.* **1986**, *25*, 4108.

(18) Karandinos, A.; Nan, S.; Mays, J. W. *Macromolecules* **1991**, *24*, 2007.

(19) Yee, L. H.; Coote, M. L.; Chaplin, R. P.; Davis, T. P. *J. Polym. Sci. A, Polym. Chem.* **2000**, *38*, 2192.

(20) Beuermann, S.; Buback, M.; Davis, T. P.; Gilbert, R. G.; Hutchinson, R. A.; Kajiwara, A.; Klumperman, B.; Russell, G. T. *Macromol. Chem. Phys.* **2000**, *201*, 1355.

(21) Beuermann, S.; Buback, M.; Davis, T. P.; Gilbert, R. G.; Hutchinson, R. A.; Olaj, O. F.; Russell, G. T.; Schweer, J.; Van Herk, A. M. *Macromol. Chem. Phys.* **1997**, *198*, 1545.

(22) Buback, M.; Gilbert, R. G.; Hutchinson, R. A.; Klumperman, B.; Kuchta, F.-D.; Manders, B. G.; O'Driscoll, K. F.; Russell, G. T.; Schweer, J. *Macromol. Chem. Phys.* **1995**, *196*, 3267.

(23) Hutchinson, R. A.; Beuermann, S.; Paquet, D. A.; McMinn, J. H. *Macromolecules* **1997**, *30*, 3490.

(24) Suddaby, K. G.; Maloney, D. R.; Haddleton, D. M. *Macromolecules* **1997**, *30*, 702.

(25) Kukulj, D.; Davis, T. P. *Macromol. Chem. Phys.* **1998**, *199*, 1697.

(26) (a) Heuts, J. P. A.; Gilbert, R. G.; Radom, L. *Macromolecules* **1995**, *28*, 8771. (b) Heuts, J. P. A.; Sudarko; Gilbert, R. G. *Macromol. Symp.* **1996**, *111*, 147. (c) Heuts, J. P. A.; Pross, A.; Radom, L. *J. Phys. Chem.* **1996**, *100*, 17087. (d) Heuts, J. P. A. In *Handbook of Radical Polymerization*; Matyjaszewski, K., Davis, T. P., Eds.; Wiley-Interscience: New York, 2002; p 1.
(27) Vana, P.; Yee, L. H.; Barner-Kowollik, C.; Heuts, J. P. A.; Davis, T. P. *Macromolecules* **2002**, *35*, 1651.
(28) Beuermann, S.; Buback, M. *Prog. Polym. Sci.* **2002**, *27*, 191.
(29) Gridnev, A. A.; Cotts, P. M.; Roes, C.; Barth, H. *J. Polym. Sci., Polym. Chem.* **2001**, *2001*, 1099.
(30) Smirnov, B. R.; Morozova, I. S.; Marchenko, A. P.; Markevich, M. A.; Pushchaeva, L. M.; Enikolopyan, N. S. *Dokl. Akad. Nauk SSSR* (*Engl. Transl.*) **1980**, *253*, 891.
(31) Smirnov, B. R.; Plotnikov, V. D.; Ozerkovskii, B. V.; Roshchupkin, V. P.; Yenikolopyan, N. S. *Polym. Sci. USSR* **1981**, *23*, 2807.
(32) Fraser, R. R.; McGreer, D. E. *Can. J. Chem.* **1961**, *39*, 505.
(33) Proton NMR spectra of dimethyl mesaconate and dimethyl citraconate are available on-line at the SDBS database: http://www.aist.go.jp/RIODB/SDBS/menu-e.html.

MA020719M